Design of High-Efficiency GaAs Solar Cells Based on TCAD 2D Numerical Simulations

Diseño de celdas solares de GaAs de alta eficiencia basadas en simulaciones numéricas TCAD en 2D

César A. Palacios A. [1], Noemi Guerra [2], Marco Guevara [3], Felice Crupi [4]*
[1] Facultad de Ingeniería, Universidad Nacional de Chimborazo, [2] Departamento de Investigación, Universidad Tecnológica de Panamá, [3] Facultad de Ingeniería, Universidad Politécnica de Chimborazo, [4] DIMES, Universidad de la Calabria
[1] cesar.palacios@unach.edu.ec, [2] noemi.guerra@utp.ac.pa, [3] m.guevara@dimes.unical.it, [4] f.crupi@dimes.unical.it

Resumen– *Este trabajo presenta varias simulaciones numericas realizadas para optener un modelo optimizado de celdas solares de ALGaAs-GaAs, usando el simulador TCAD Sentaurus. Para llegar al modelo final, primero se realizó una revisión actualizada al estado del arte y se proporciona una derivación teorica de caracteristicas para este tipo de celdas solares. Con el fin de introducir a las celdas solares tipo tandem, se realiza una comparación entre un modelo con un contacto inferior completamente metalizado y luego un modelo con un contacto de 5μm. Para resolver la parte eléctrica y óptica de la celda solar, son usados varios métodos por Sentaurus. El métdo de trasnferencia de matrices y el método Raytracing, son utilizados para resolver la parte óptica, en cambio para la parte eléctrica se resuelven las ecuaciones de semiconductores, principalmente las ecuaciones de Poisson. Al final del trabajo se realiza una fase de optimización de la celda, para así tener un óptimo desempeño de la celda, se analiza el efecto de grosor y dopaje en las diferentes capas de la celda.*

Palabras claves– *Celdas solares AlGaAs-GaAS, Energía solar, simulaciones numéricas, TCAD, Sentaurus, Método de transferencia de matrices, Raytracing*

Abstract– *This paper presents several numerical simulations to obtain an optimized model for AlGaAs-GaAs solar cell, using the TCAD simulator of Sentaurus. First an updated review of the state of the art in the development of GaAs solar cell is provided, with emphasis on the AlGaAs-GaAs cells. Secondly, a set of theoretically derived characteristics is given for this type of solar cells. Then, a comparison between two solar cell architectures is considered, one with a full metalized back contact and other with a back contact of 5μm. To resolve the optical and electrical characteristics of the solar cell, some methods can be used by TCAD Sentaurus. The transfer matrix method (TMM) and the Raytracing approach are implemented to solve the optical part of the cell. Instead, for the electrical part, the resolution of the semiconductor equations, principally the Poisson equation, was computed. At the end of the work an optimization phase of the solar cell was made, in order to search the technological parameters leading to optimal performances of the cells, the effects of the doping level and the thicknesses of the base, bsf and emitter layers were also investigated.*

Keywords– *AlGaAs-Gas solar cell, solar energy, photovoltaics, numerical simulations, TCAD, Sentaurus, transfer matrix method, raytracing*

1. Introduction

The incident radiation from the sun is the basis for all life on the Earth. Solar energy generation is the availability of transform sun light into any other form of energy, e.g. green plants, and some other organisms use sunlight to synthesize foods from carbon dioxide and water in a process called photosynthesis. Humans cannot directly transform the energy, but we use devices to mechanically or chemically convert it.

Photovoltaic energy conversion in general words can be explained as the technology that generates electrical power measured in Watts(W) from semiconductors when they are illuminated by photons [5].

The work is focused on to get the optical and

electrical characteristics of two-dimensional(2D) single junction GaAs solar cell by using numerical simulations to develop and optimize semiconductor processing technologies and devices by means of Sentaurus *Technology Computer-Aided Design (TCAD)* tools.

The process starts defining the geometrical structure and materials, then we obtain the generation profiles and insert those result in a process, called *V isual*, that extracts and filters the data to show graphics, curves, band diagrams and profiles of the figures of merit to evaluate the solar cell performance. Finally, in order to get an optimized GaAs solar cell, additional experiments have been done, changing the geometric and doping levels of the layers of the cell.

1.1 GaAs Solar cell features

Solar cell based in AlGaAs-GaAs alloys are used at high-efficiency, they are related with the semiconductors of the III-V group, because these are made with compounds of elements from the column III and V in the periodic table. *ttaAs* is alloyed with *Al* to give the ternary compound $Al_xtta_{1-x}As$; compound that was analized and simulated in this paper.

The characteristics of Gallium Arsenide (GaAs) have made of it, a photovoltaic material of interest. The bandgap of GaAs is 1.42 eV at 300K. This is very nearly ideal for a photovoltaic device operating in our solar spectrum. Therefore, GaAs solar cells can operate at higher temperatures than silicon (Si) cells and are expected to be very radiant resistant, furthermore GaAs solar cells have higher electron mobility and higher saturation velocity[6].

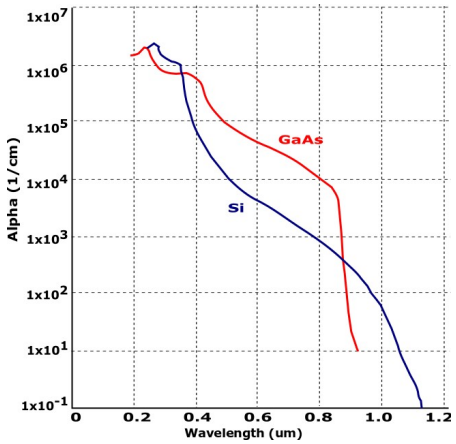

Figure 1. Photovoltaic effect in a GaAs solar cell.

The direct bandgap of the GaAs causes in the material a high optical absorption coefficientα. This coefficient indicates how far the light of a particular wavelength can penetrate before that it have been absorbed. In a material with a low absorption coefficient, light is poorly absorbed, additional if the material is thin, it can be seen as a transparent layer[1]. The α for GaAs rises very steppy at the band edge ($\lambda = 0.88$ μm) to values grater than $10^4 cm^{-1}$, in contrast with the gradually rise of the absorption coefficient for silicon. We can see the curves of optical absorption vs. wavelength for the both of materials in Figure 1.

1.2 Simulation Software

Sentaurus is a TCAD software, developed by Synopsys, which solves the diffusion and transport equations, to modeling the structural properties and electrical behavior of semiconductor devices. All leading semiconductor companies use Synopsys TCAD tools throughout the technology development cycle. TCAD tools allow engineers to explore new design alternatives, test the quality of passivation layers, varying the lifetimes of charges executing simulations. Also is possible to evaluate, characterize, and optimize the process.

2. GaAs solar cell based Analysis

In 1970 a Russian group reported a heterojunction solar cell consisting of a p-type emitter of $tta_{1-x}Al_xAs$, grown on a *n-type* base of *ttaAs*. It means that the layer can be made thick and heavily doped reducing the series resistance and reduce the surface recombination.[2].

The solar cell that is analyzed and simulated is a GaAs based. It use two layers of an antireflective coating (ARC), the first one is a MgF_2 layer and the second one a TiO_x layer. The bulk is GaAs based with two differents levels of doping, dividing the bulk in a emitter and a base. To reduce the recombination losses, a front surface field (fsf), is used, and a back surface field (bsf) made of *AlttaAs*. A preliminary sketch of the solar cell is shown in Figure 2.

2.1 The architecture of GaAs-AlGaAs solar cell

TCAD simulator requires some dimensions: lengths, shape geometry, mesh, and doping profiles. The bandgap of GaAs is close to the optimum E_g for single junction solar cells whose maximum efficiency is above 30% [8].A sketch of the model is shown in Figure 2. Note that the structure has been studied under AM1.5 solar spectrum,

with $P = 0,\ 1W/cm^2$, and at room temperature $T = 300K$.

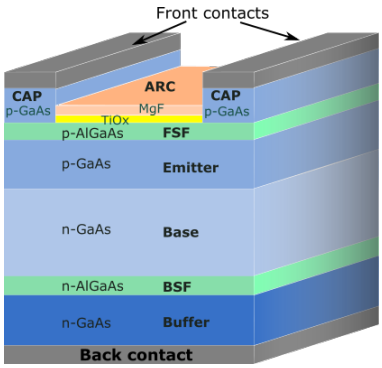

Figure 2. Schematic of the GaAs solar cell. Electrons and holes are extracted through the front contact and the back contact.

The GaAs solar cell structure includes a "buffer layer" of n-doped GaAs, even though such a buffer layer is not needed theoretically. It was been included for practical reasons, because the doping level and the surface quality of the GaAs wafer actually available have been found to lack adequate control. Furthermore, the higher n^+ doping level in the GaAs substrate rather than in the n^- doped buffer layer allow easier fabrication of the back contact. The important characteristics for GaAs cells are: 1) a thin (AlGaAs) fsf layer less than $0,\ 5\mu m$ and 2) a diffused electrical junction less than $0,\ 5\mu m$ deep. This ensures low optical absorption losses and minimizes the surface-recombination characteristic of GaAs surfaces and the latter ensures increased radiation hardness[3].

The detail of thickness and doping levels from Figure 2, used for simulations are specified in Table 1.

Table 1. Details of solar cell structure to simulate

Region	Material	Thickness $[\mu m]$	Doping $[cm^{-3}]$
cap	GaAS	0.2	$-1,00e^{19}$
fsf	AlGaAs	0.04	$-2,00e^{18}$
emitter	GaAs	0.8	$-9,00e^{17}$
base	GaAs	3.2	$1,00e^{17}$
bsf	AlGaAs	0.2	$5,00e^{18}$
buffer	GaAs	0.35	$2,00e^{18}$
contacts	Aluminum	1	

2.2 Simulation domains and mesh definition

The method of simulation adopted for this work consists in evaluate independently the optical and electric simulations. For instance, the meshing resolution size should be much finer than the needed to solve the electrical behavior, in the device. Even the considerations of sizing and shape are different for each one. Regarding the optical analysis, it is important considering the effects of surface texturing over the charge collection but is sufficient enough to take a look only in a portion that characterized the full surface roughness instead of unnecessary modeling the whole device area. Taking the case of a solar cell featuring finger as front contact and a back contact in the whole rear, it is sufficiently just modeling a small respective portion of the structure, that is typically half of the symmetry element in two dimensions, and a quarter of the symmetry element in three dimensions as is shown in Figure 3.

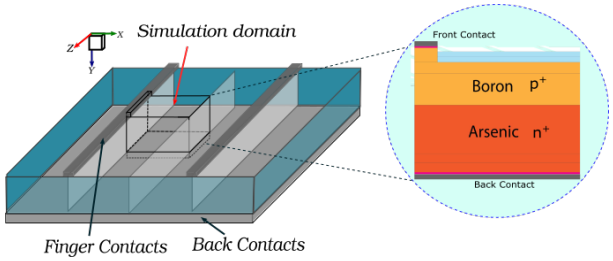

Figure 3. Simulation domain. Left side, 3D simulation domain selection. Right side, 2D resulting simulation domain.

The electric-simulation domain is usually bigger than the optical one and requires another meshing strategy. The meshing procedure starts by creating a coarse grid in the whole structure followed by the addition of finer meshing refinements near to the junctions and metal contacts, as well as, in the uppermost part of the device, where most of the generation occurs. In Figure 4, is sketched a mesh for the simulation domain from Figure 3.

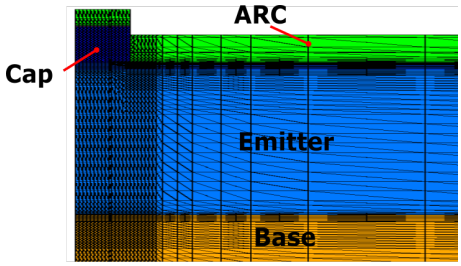

Figure 4. Mesh definition for a piece of the simulation domain.

3. Optical Simulation Results

In order to obtain the optical characteristics in the simulation, we have to calculate the topics listened below:

- Optical intensity, absorbed photon density and optical generation rate usin TMM solver.
- Optical intensity, absorbed photon density and optical generation rate usin Raytracing solver.
- Integrated optical generation rate, which is used subsequently in Sentaurus Visual to compute the photogenerated current density $J_{ph}(mA/cm^2)$.
- Reflectance, transmitance and absorbance.
- Terminal current density $J(mA/cm^2)$

3.1 Optical generation profiles

Simulation of PV devices under illumination requires a source file numerically coupling, by Sentaurus TCAD, to the simulation domain that contains the geometry structure, mesh and optical physics information of materials to calculate the photogeneration rate of electron-hole pairs by solving the transport equations. The solar spectrum file sweeps the wavelength of incident sunlight from (300 nm) up to (1200 nm) using the conventional one-sun AM1.5G spectrum with an incident power of 1000 W m^{-2}, defined in a file with two-column format. The first column contains the wavelength in μm and the second one contains the intensity in W cm^{-2}. This file is calculated based on the air mass 1.5 global tilted irradiance, by the spectral radiation model called SMARTS v 2.9.2 with inputs chosen per international standard IEC 60904-3-Ed2 [4], as shown in . Figure 5. The simulator also calculates the reflectance, transmittance, and absorbance as a function of the wavelength (λ).

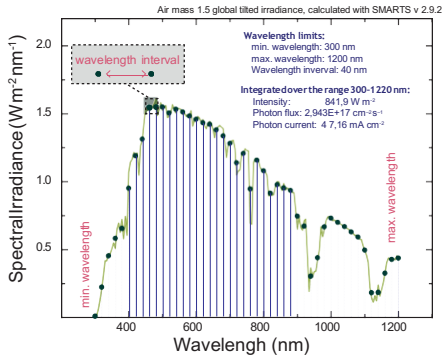

Figure 5. Air mass 1.5 global tilted irradiance.

The absorption coefficient α is computed from κ and wavelength λ according to $\alpha = \frac{4\pi}{\lambda} \cdot \kappa$. It determines how far inside a material the light, with a particular wavelength, can penetrate before being absorbed to create electron-holes pairs. Semiconductor materials can only absorb energy from particles that have sufficient energy to excite an electron from the valence band to the conduction band.

3.2 Optical results using the Transfer Matrix Method (TMM)

The TMM solver computes the optical intensity by taking into account the interference effects due to standing waves or by neglecting the phase and, therefore, the interference effects. Neglecting the phase is valid only for large layer thicknesses (depending on the extinction coefficient). It is assumed, in the model of the optical generation rate, monochromatic plane waves with arbitrary angles of incidence and polarization states penetrating a number of planar, parallel layers.

These matrices are functions of the complex wave impedances Z_j given by $Z_j = n_j \cdot cos(\theta_j$ in the case of E polarization (TE) and by $Z_j = n_j/(cos(\theta_j)$ in the case of H polarization (TM). Here, n_j denotes the complex index of refraction and θ_j is the complex counterpart of the angle of refraction $(n_0\, sin(\theta_0 = n_j\, sin(\theta_j))$.

In the Figure 6 and Figure 11, are presented the optical generation rate an the optical generation profile in GaAs solar cell as a function of depth. Two simulations have been done, one for the case in which the whole surface is completely metallized and the other one for the case which considers a short contact.

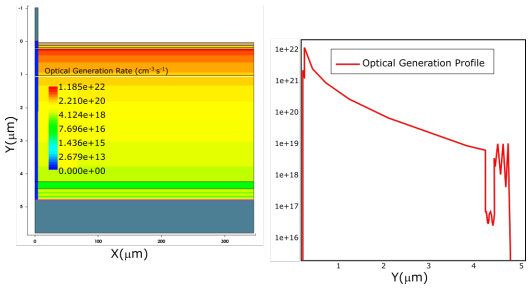

Figure 6. Optical generation rate and optical generation profile for a full metallized rear contact.

The blue-colored region below the front contact finger indicates that the optical generation rate is zero in the region since it is not illuminated. The optical generation profile shows that the optical generation rate decreases as a function of depth.

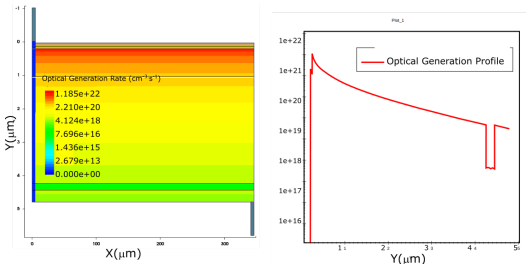

Figure 7. Optical generation rate and optical generation profile within $5\mu m$ back contact.

In both of the results we have present the effect of the bsf as a hole at the end of the curve. In the case of full metallized rear contact, it presents the effect of a full aluminum metallized rear contact as a kind of perturbations near to the back contact. In the other case, the effect of the rear contact is almost imperceptible. In order to have a confront between the two optical generation profiles, the data is then post process using MatLab. The Figure 8 shows the confront between the two optical generation profiles.

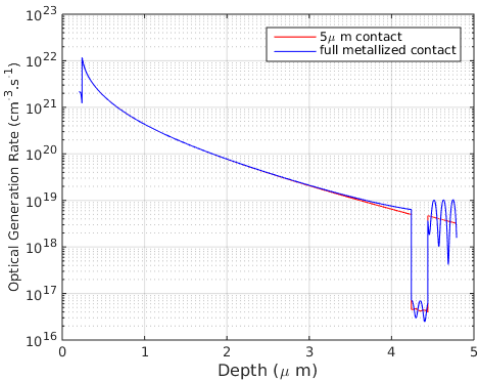

Figure 8. Optical generation profiles TMM-based.

3.3 Optical results using the "Raytracer" algorithm

In the section of the simulator called Sentaurus Device, each material has a complex refractive index section defined in the parameter file. The raytracer solver uses a recursive algorithm that starts with a source of rays and it builds a binary tree that tracks the transmission and reflection of the rays. A reflection-transmission process occurs at interfaces with refractive index differences.

The obtained results are shown in Figure 10 and Figure 9. In the region over and under the cell there are also simulated the pieces of ambient that are used as sensor for the rays. The rays starts at a height of $2,\ 5\mu m$ over the cell.

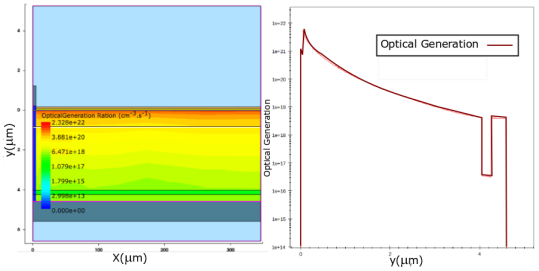

Figure 9. Optical generation rate and optical generation profile for a full mettalized rear contact.

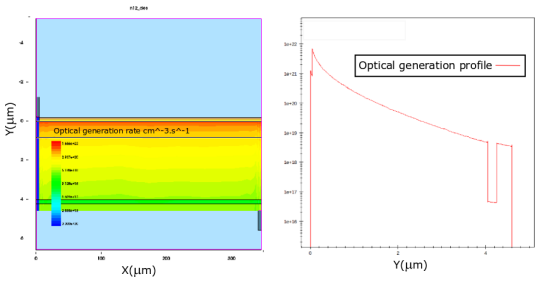

Figure 10. Optical generation rate and optical generation profile within $5\mu m$ back contact.

The results of Raytracing are in the same range that the results of the TMM process. With this results we can say that the both of the methods can work for the model of solar cell under the optical analysis. In the Raytrace 2D simulation there are oscillations and random values of optical generation due to the nature and behavior of the incident rays. Finally, in order to have the effect of the metallization on the cell, a confront between the optical generation with full metallized back contact and the contact of $5\mu m$, is presented.

4. Electrical Simulation Results

The *I–V* characteristics of the illuminated solar cell are simulated by ramping the anode voltage. There are two ramps, the goal voltage for the first ramp should be less than V_{mpp}. The goal voltage for the second ramp should be greater than V_{oc}. Since both P_{mpp} (and, therefore, V_{mpp}) and V_{oc} are unknown before starting the simulation, the goal voltages for both ramps are chosen iteratively. Initially, the simulation runs with a guessed value of V_{mpp} and then looks at the computed

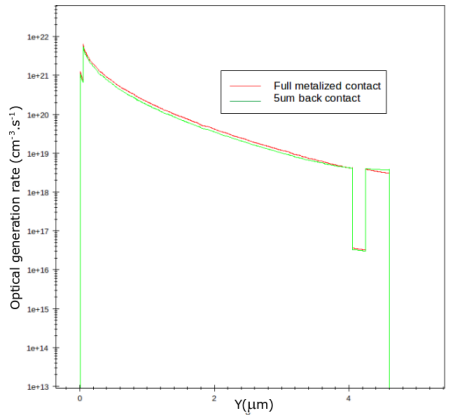

Figure 11. Optical generation between the full metalized back contact against 5 μm back contact

P–V characteristics to establish a better approximation for V_{mpp}.

4.1 Impact of the total width in the solar cell

The first experiment is to change the total pitch of the cell, to determine the best width to continue with the others optimization experiments. **??** shows the efficiency and FF against the length of the pitch. According to Figure 12, the best length is 325μm, the efficiency tend to go up until the 325μm. Around the 325μm the efficiency becomes constant but the Fill Factor decreases, as show in Figure 13.

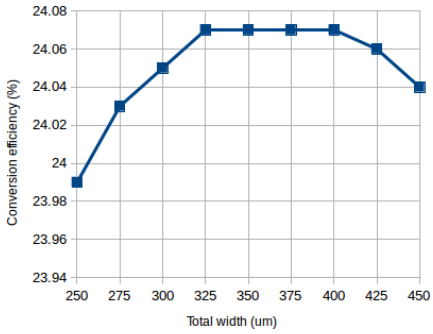

Figure 12. Convertion efficiency vs cell width

The best trade-off between the conversion efficiency η and the Fill Factor FF take place at a total width of 325μm.

4.2 Impact of the FSF layer in the solar cell

The Figure 15 shows the behavior of J_{sc} as a function of the AlGaAs fsf layer thickness, in order to determine the advantage of using thin FSF layers. Two different

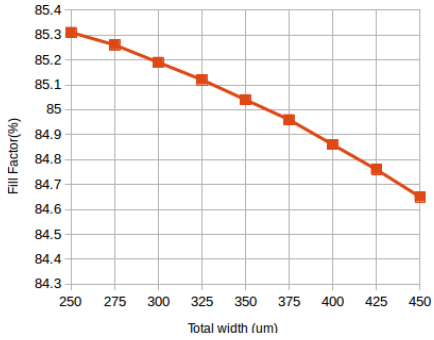

Figure 13. Effects of the width in the solar cell performance.

experiment have been done about the FSF layer, one rewarding the doping of the layer and the other one changing the thickness of the fsf layer, Figure 14.

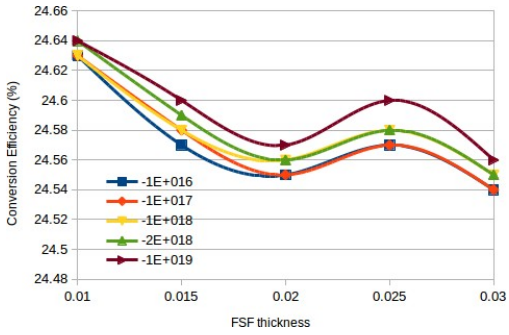

Figure 14. Conversion efficiency

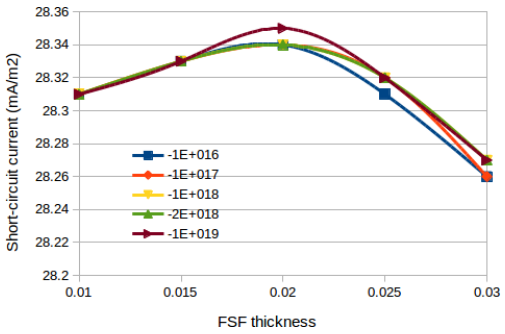

Figure 15. Short-circuit current

4.3 Impact of the base layer

To study the influence of the base layer,the thickness of the latter is varied between 1μm and 9μm [7] and the doping level from $1 \times 10^{16} cm^{-3}$ to $2 \times 10^{16} cm^{-3}$. The other parameters are configured as the Table 2 shows.

Table 2. Layer configuration for the GaAs solar cell

~~Region~~	~~Thickness~~ [μm]	~~Doping~~ [cm^{-3}]	~~width~~[μm]
cap	0.2	$-1,00e^{19}$	5
fsf	0.04	$-2,00e^{18}$	325
emitter	0.8	$-9,00e^{17}$	325
bsf	0.2	$5,00e^{18}$	325
buffer	0.35	$2,00e^{18}$	325

According to the Figure 16, the best conversion efficiency is around $2\mu m$, but depending on the doping, it has different values. For a doping level of 1e+16 we have an efficiency around 22.5%. Then with a doping level of 2e+17 and the thickness of $2\mu m$ the conversion efficiency of the cell arrives to his maximum value, 24,7%. But if the doping continues to increment, the efficiency decrements, as the example, with a doping level of 5e+17 the efficiency is 23,5%.

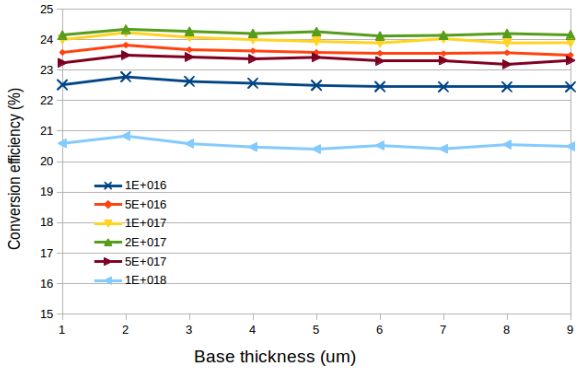

Figure 16. Base thickness effect.

Photons with lower energy which are absorbed with base layer are sensitive to the layer thickness and absorption coefficient. The base layer thick is $2\mu m$, enough to absorb as much photons as possible and lower doing concentration level in order to improve the collection of photo-generated carriers. Figure 17 shows the effect of doping level on the conversion efficiency.

4.4 Impact of the Emitter layer

In one hand, the intention of the heavily doping in the emitter layers is to improve its conductivity. But, in the other hand, the thickness of the base and the emitter should exceed the incident photon's absorption length.

Figures Figure 18 and Figure 19 show the efficiency versus the doping and thickness of the emitter layer. The

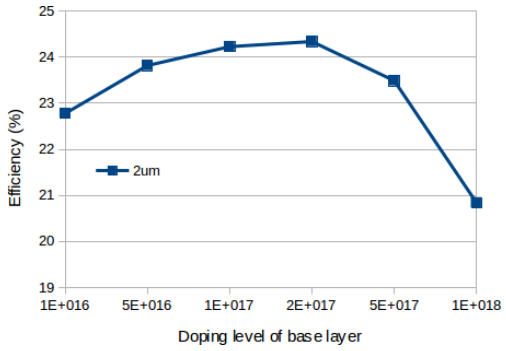

Figure 17. Base dopping level effect.

doping concentration level of the base and the emitter thickness change quickly the efficiency of the cell.

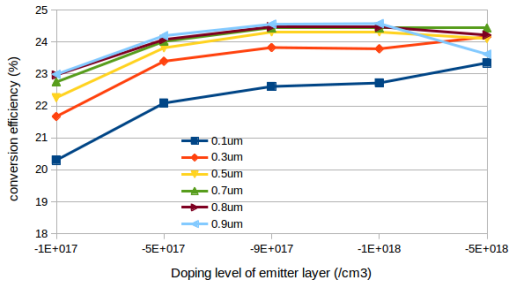

Figure 18. Emitter doping level effect.

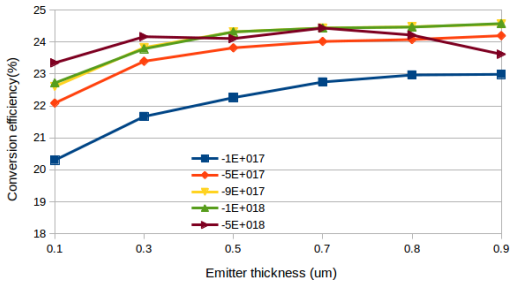

Figure 19. Thickness of emitter effect.

5. Optimized model

The optimized geometrical parameter and the results are presented in the Table 3 and Table 4, respectively.

5.1 Light J-V Characteristics

The I-V and P-V characteristics of the illuminated cell are presented in Figure 20. The power density of the cell is also computed using $P = JV$. The fill factor and

Table 3. Optimized GaAs solar cell results

Region	Thickness $[\mu m]$	Doping $[cm^{-3}]$	width$[\mu m]$
cap	0.2	$-1,00e^{19}$	5
fsf	0.02	$-2,00e^{18}$	325
emitter	0.9	$-1,00e^{18}$	325
bsf	0.2	$5,00e^{18}$	325
buffer	0.35	$2,00e^{18}$	325

Table 4. Results of the optimized GaAs solar cell

Contact (μm)	J_{sc} $[mA/cm^2]$	$V_{oc}[V]$	J_{ph} $[mA/cm^2]$	FF(%)	$\eta(\%)$
5	28.27	1.024	29.01	84.56	24.47
325	28.3	1.023	29.09	84.85	24.58

the power conversion efficiency are also computed. The obtained values for the 2D optimized cell, considering the full metalized contact approach are, $J_{sc} = 28,3 mA/cm^2$ and $J_{ph} = 29,09 mA/cm^2$, instead of, for the $5\mu m$ back contact approach, the results are, $J_{sc} = 28,27 mA/cm^2$ and $J_{ph} = 29,01 mA/cm^2$.

The value of $J_{sc} < J_{ph}$ because all the photon generated carriers cannot be collected at the electrodes, due to recombination losses.

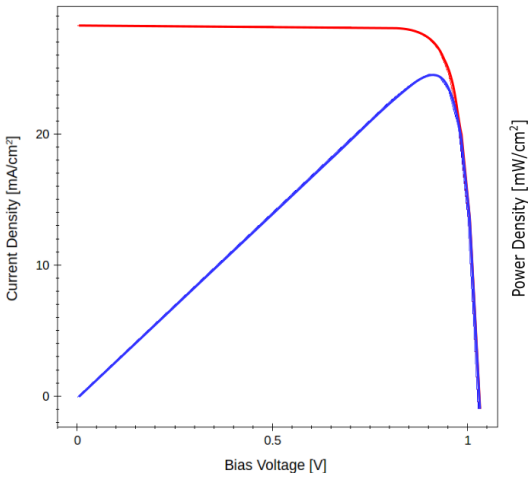

Figure 20. Light I-V and P-V characteristics of full metalized back contact GaAs solar cell

6. Conclusion

TCAD modeling is a powerful and helpful tool that reduce the time of manufacturing and speed up the optimization processes of solar cell. It allows test the concept designs before the implementation, improve the old ones or simply optimized a designed model.

An optimized AlGaAs-GaAs solar cell was designed. The two approaches, were simulated. The first one, considered a full metallized back contact and the second one using a smaller back contact of $5\mu m$ in order to be implemented as a top cell in a tandem solar cell approach. The performance of the GaAs solar cells agrees with theoretical expectations. Some special characteristics that makes this kind of cells specials are the high efficiency and the capability to develop thinner lower weight solar cells.

Two important characteristics are needed for GaAs solar cell, a thin AlGaAs fsf layer less than $0.5\mu m$ thick and a diffused electrical junction less than $0.5\mu m$ deep, to ensure optical absorption losses and minimizes the surface recombinations. The characteristics of the full metalized back contact are better because of the bigger area of the back contact to collect electrons.

References

[1] "The absorption of radiation in solar stills," *Solar Energy*, vol. 12, no. 3, pp. 333 –346, 1969,
, ISSN: 0038-092X.

[2] J. Woodall and H. Hovel, "High-efficiency ga1- x al x as–gaas solar cells," *Applied Physics Letters*, vol. 21, no. 8, pp. 379–381, 1972.

[3] R Loo, G. Kamath, and R. Knechtli, "Radiation damage in gaas solar cells," 1980.

[4] C. Gueymard, *SMARTS2: A simple model of the atmospheric radiative transfer of sunshine: Algorithms and performance assessment*. Florida Solar Energy Center Cocoa, FL, 1995.

[5] S. S. Hegedus and A. Luque, "Status, trends, challenges and the bright future of solar electricity from photovoltaics," *Handbook of photovoltaic science and engineering*, pp. 1–43, 2003.

[6] A. Luque and S. Hegedus, *Handbook of photovoltaic science and engineering*. John Wiley & Sons, 2011.

[7] M Abderrezek, F Djahli, M Fathi, and M Ayad, "Numerical modeling of gaas solar cell performances," *Elektronika ir Elektrotechnika*, vol. 19, no. 8, pp. 41–44, 2013.

[8] C. Zhang, *High Efficiency GaAs-based Solar Cells Simulation and Fabrication*. Arizona State University, 2014.